Limnol. Oceanogr., 59(2), 2014, 560–577

doi:10.4319/lo.2014.59.2.0560

Increased cellular brevetoxins in the red tide dinoflagellate *Karenia brevis* under CO_2 limitation of growth rate: Evolutionary implications and potential effects on bloom toxicity

D. Ransom Hardison,[1,*] William G. Sunda,[1] Patricia A. Tester,[1] Damian Shea,[2] and R. Wayne Litaker [1]

[1] National Oceanic and Atmospheric Administration, National Ocean Service, Center for Coastal Fisheries and Habitat Research, Beaufort, North Carolina

[2] Department of Biology, North Carolina State University, Raleigh, North Carolina

Abstract

Karenia brevis blooms impair human health, marine ecosystems, and coastal economies in the Gulf of Mexico via their production of carbon-based neurotoxins (brevetoxins), which contain no nitrogen (N) or phosphorus (P). N and P limitation of growth rate substantially increases brevetoxins in this dinoflagellate, consistent with predictions of the carbon nutrient balance (CNB) hypothesis. This hypothesis further predicts that an increase in carbon-based brevetoxins should not occur if growth rate is limited by carbon dioxide (CO_2). We tested this prediction by examining the effect of CO_2 limitation of *K. brevis* growth rate on cellular brevetoxins. In contradiction to the prediction of the CNB hypothesis, brevetoxins normalized to cell carbon were on average 81% higher in CO_2-limited cells growing at a rate of 0.1 d^{-1} than in cells growing at their maximum rates (0.4–0.5 d^{-1}). This increase in brevetoxin : C values in the CO_2-limited cells, however, was 23–42% lower than that previously observed for comparable growth rate limitation by phosphate. The CO_2-limited cells also exhibited 40% higher cellular N : C and 60–100% higher chlorophyll *a* : C than observed in P-limited cells at equivalent growth rates. These effects were likely due to the up-regulation of the cell's CO_2-concentrating mechanism under CO_2 limitation, which increased the demand for photosynthetically produced adenosine-5′-triphosphate. The results indicate that anthropogenic increases in CO_2 concentrations in surface ocean waters are likely to increase the toxicity of *K. brevis* blooms due to potential increases in bloom biomass yield and to a greater likelihood that dense blooms will become N or P limited rather than CO_2 limited.

The red tide dinoflagellate *Karenia brevis* produces a suite of polyether neurotoxins (brevetoxins) that serve as a potent grazing defense against copepods and likely other zooplankton (Cohen et al. 2007; Hong et al. 2012; Waggett et al. 2012). Recent experiments have shown that growth rate limitation of *K. brevis* by nitrogen (N) and phosphorus (P) increase cellular brevetoxin (PbTx) concentrations (Hardison et al. 2012, 2013). This increase in cellular toxins as growth slows is evolutionarily advantageous because it should reduce grazing mortality losses (Waggett et al. 2012; Hardison et al. 2013).

In the experiments of Hardison et al. (2012, 2013), PbTxs normalized to cell volume or cell carbon increased on average two- to threefold when growth was limited by N or P (Hardison et al. 2012, 2013). The largest increase in cellular toxins occurred during the transition period from nutrient-replete to nutrient-limited growth when the imbalance between photosynthesis and growth was greatest. As the cells down-regulated their photosynthetic apparatus to bring carbon fixation and growth back into balance, the cellular toxin concentrations declined in most cases, but remained higher than observed during nutrient-replete growth. These observations conform to predictions of the carbon nutrient balance (CNB) hypothesis, first formulated for terrestrial plants (Bryant et al. 1983) but later applied to microalgae (Ianora et al. 2006). This hypothesis states that the concentration of carbon-based defense compounds should increase in plant cells and tissues in response to growth limitation by nutrients.

The above findings have significant implications for the toxicity of *K. brevis* blooms. They indicate that as *K. brevis* blooms become nutrient limited due to a high biomass demand for nutrients, they will become substantially more toxic (Hardison et al. 2012, 2013). Such blooms frequently exceed 1,000,000 cells L^{-1} along the west Florida shelf. The combination of high biomass and nutrient limitation can result in extremely toxic blooms (W. G. Sunda and K. Shertzer unpubl.).

Unpublished measurements taken during high-density *Karenia* blooms indicate that pH in surface ocean water can reach values of 8.8–9.0 (K. Steidinger pers. comm.), which corresponds to a 7- to 14-fold decrease in carbon dioxide (CO_2) concentrations caused by the bloom's high photosynthetic consumption of CO_2. Such CO_2 depletion can limit algal growth during blooms (Riebesell et al. 1993). The potential for nutrient vs. CO_2 limitation of growth raises an interesting question concerning the toxicity of high-density blooms. The CNB hypothesis postulates that, unlike nutrient limitation of growth rate, growth limitation by low CO_2 or low light will decrease concentrations of carbon-based defensive toxins that contain no N or P or

* Corresponding author: rance.hardison@noaa.gov

will leave toxin levels unchanged (Bryant et al. 1983). Brevetoxins contain no N or P and fall into this category. Thus, based on the CNB hypothesis, cellular brevetoxins should not increase in response to CO_2 limitation.

The goal of this study was to test this prediction by determining the extent to which growth limitation by CO_2 affects the PbTx content in otherwise nutrient-replete *K. brevis* cells compared with the toxin increases observed in N- or P-limited (and CO_2-sufficient) cultures. Understanding this relationship has important implications for predicting the effects of anthropogenic increases in nutrient and CO_2 concentrations on bloom growth and toxicity and associated adverse effects. Brevetoxin production by these blooms cause neurotoxic shellfish poisoning and respiratory distress in humans (Watkins et al. 2008; Backer 2009). These blooms are also responsible for massive fish kills, marine mammal deaths, and significant economic losses in coastal communities (Flewelling et al. 2005; Hoagland and Scatasta 2006).

To examine the effect of CO_2 limitation on PbTx content in *K. brevis* cells, a series of experiments were conducted with nutrient-enriched batch cultures and semi-continuous batch cultures whose growth rates were decreased, respectively, to zero or 0.1 d^{-1} by low CO_2 concentrations. These results were then compared with those from nutrient- and CO_2-sufficient, semi-continuous cultures growing at their maximum rates (0.30–0.55 d^{-1}). The experiments were conducted with three different *K. brevis* strains in media containing sufficiently high nutrient concentrations to ensure that cell growth was limited by CO_2 rather than by nutrients such as N or P. Carbon dioxide concentrations computed from measured pH values were on average 8- to 13-fold lower in the CO_2-limited cultures than in the control cultures. The physiological status of the experimental cultures was examined by measuring cellular chlorophyll *a* (Chl *a*) : C and N : C for each sampling period. For comparison with other studies, brevetoxin concentrations were normalized per cell, per unit of cell volume, and as a percent of cellular carbon.

Our results showed that growth rate declined as CO_2 concentrations decreased below 2.5 μmol L^{-1} and associated pH values increased above 8.7. Brevetoxin : C increased in the CO_2-limited cells, in contrast to the response predicted by the CNB hypothesis. However, the increase was not as much as occurred at comparable low growth rate under N and P limitation. In each isolate tested, the cells still diverted more cellular carbon into PbTxs than occurred in exponentially growing, CO_2-replete cells, indicating a strong selection pressure for diversion of carbon into C-based defensive compounds even when the growth rate was limited by low CO_2 and associated low rates of C fixation.

Methods

Strains and culture conditions—Three *K. brevis* strains were examined in this study. Strains of the Center for Culture of Marine Phytoplankton (CCMP) 2228 and 2229 were obtained from the Provasoli–Guillard National Center for Marine Algae and Microbiota (East Boothbay Harbor, Maine). Strain SP3 was kindly provided by Ed Buskey of University of Texas Marine Science Institute. Experimental cultures were grown in media prepared from Gulf Stream seawater (salinity 36) that had been filtered through 0.2 μm pore Nuclepore filters to remove particles. The culture medium contained added vitamins (0.074 nmol L^{-1} vitamin B_{12}, 0.4 nmol L^{-1} biotin, and 60 nmol L^{-1} thiamine), Na_2SeO_3 (10 nmol L^{-1}), and an ethylenediaminetetraacetic acid (EDTA) trace metal buffer system (100 μmol L^{-1} EDTA, 1 μmol L^{-1} FeEDTA, 50 nmol L^{-1} $MnCl_2$, 40 nmol L^{-1} $CuCl_2$, 100 nmol L^{-1} $ZnSO_4$, and 40 nmol L^{-1} $CoCl_2$; Sunda et al. 2005). It also contained 128 μmol L^{-1} $NaNO_3$ and 8 μmol L^{-1} NaH_2PO_4 to generate a Redfield N : P of 16 : 1. Media were sterilized by microwave treatment (Keller et al. 1988). Once inoculated, cultures were placed in a Percival Scientific model I-36VLX incubator maintained at a constant temperature of 23°C and on a daily 14 : 10 light : dark cycle to simulate summer light conditions. Photosynthetically active radiation was provided at a light-saturating intensity of 120 μmol quanta m^{-2} s^{-1} via vertically mounted fluorescent Duro-test Vita-lites™ (Vargo 2009). Light intensity was measured with a Biospherical Instruments QSL-100 4π wand-type light meter. Culture pH was measured throughout each experiment using a pH meter (Thermo Orion 3 Star Plus) equipped with a Ross ultracombination pH electrode (resolution, 0.001; relative accuracy, $\pm$0.002 pH units). A two-point calibration was performed daily before and after analysis using certified National Institute of Standards and Technology traceable pH 7 and 10 buffers.

In a first set of experiments cells were grown semi-continuously under CO_2-sufficient and CO_2-limiting conditions. To initiate the CO_2-sufficient cultures, cells were inoculated into fresh media and were diluted every 2–7 d at an average dilution rate equal to their maximum growth rates, which varied from 0.37 to 0.50 d^{-1} depending on the isolate. The growth of these cultures was maintained at their maximal rates by diluting them with new medium before the onset of CO_2 limitation of growth rate (*see* Figs. 1A, 2A, 3A). The lack of CO_2 limitation was indicated by the ambient computed CO_2 concentrations of 5–15 μmol L^{-1}, which correspond to pH values of 8.5–8.1. The dilution process was continued until maximal steady state growth of each culture was observed for several weeks. Once this steady state growth was achieved, each culture was divided to form two new diluted cultures. One culture was grown under the same semi-continuous dilution regime as before to maintain maximal nutrient- and CO_2-sufficient growth rates (*see* Figs. 1A, 2A, 3A). The other half was allowed to grow into early stationary phase, where the biomass was sufficiently high to cause CO_2 limitation of the cellular growth rate. As soon as the cultures reached early stationary phase, new medium was added every 2–3 d at an average dilution rate of 0.1 d^{-1}, which allowed maintenance of continuous CO_2-limited growth at a rate of 0.1 d^{-1}. The average measured pH in these cultures was 8.89–8.91, which corresponded to CO_2 concentrations of 1.2 to 1.3 μmol L^{-1} (Table 2). These low CO_2 concentrations are consistent with CO_2 limitation of growth. Cell concentrations, mean volume per cell, cell Chl *a*, cell C and

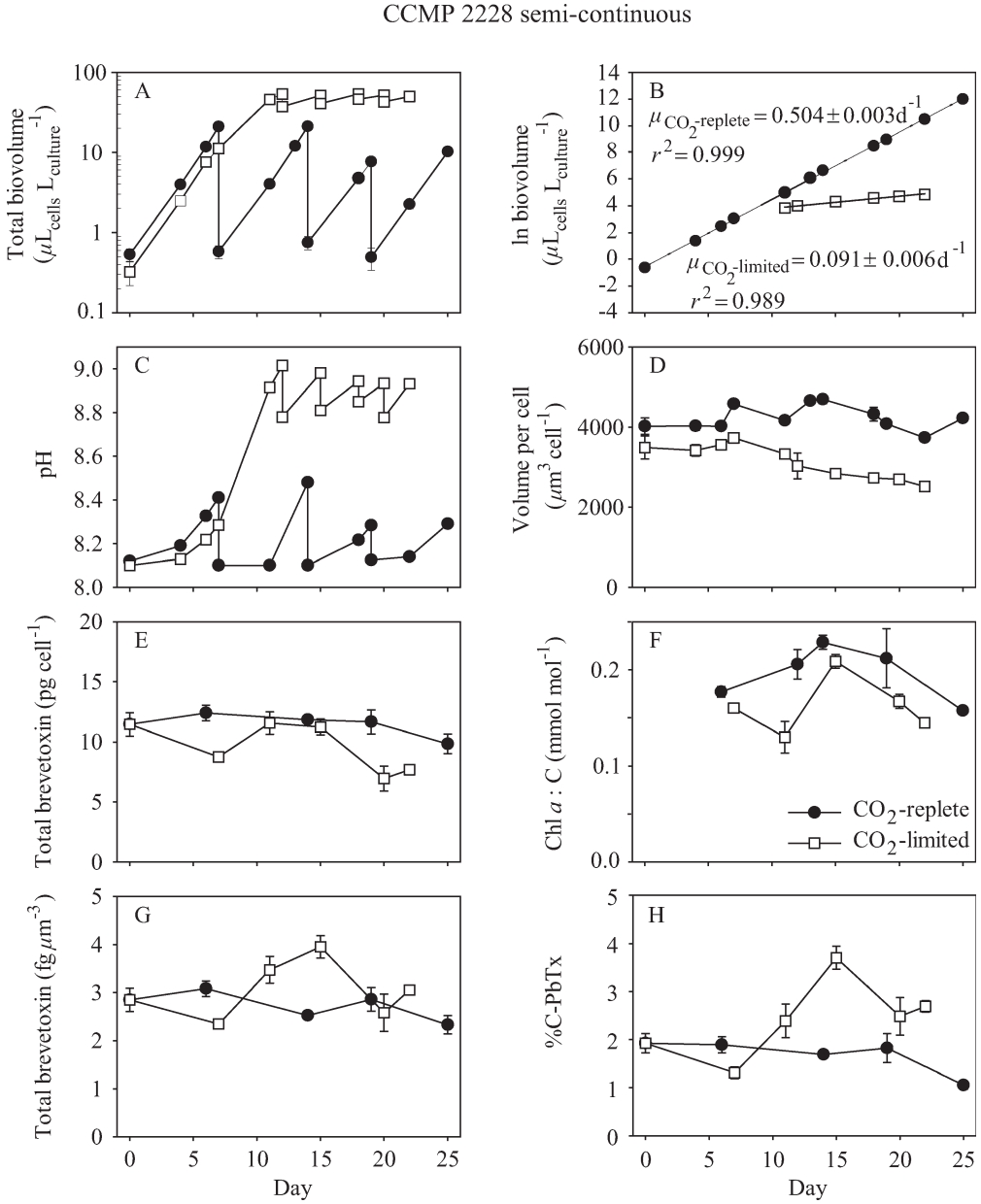

Fig. 1. Time-dependent results for semi-continuous batch cultures of *Karenia brevis* strain CCMP 2228 grown under nutrient-sufficient CO_2-replete and CO_2-limited conditions: (A) growth curves of total culture biovolume ($\mu L_{cells} L_{culture}^{-1}$) vs. time (d), (B) curves for the natural log (ln) of total biovolume vs. time correcting for culture dilution (Sunda et al. 2007), (C) culture pH vs. time (d), (D) mean volume per cell (μm^3 cell^{-1}), (E) total brevetoxins per cell (pg cell^{-1}), (F) Chl *a* normalized to cell carbon (mmol mol^{-1}), (G) brevetoxins normalized to cell volume (fg μm^{-3}), (H) brevetoxins as a percentage of cellular carbon (%C-PbTx). Error bars represent the standard deviation of three replicate measurements, except in panels F and H, where the cell carbon values were measured in duplicate.

N, and brevetoxins were measured for each sampling period as described below. Specific growth rates were determined from time-dependent changes in total cell volume (Sunda et al. 2007).

In a second set of experiments, semi-continuous cultures of the three isolates growing at their maximum nutrient- and CO_2-sufficient rates were diluted with new media to form two parallel sets of cultures. The first set was maintained as before at their maximum growth rate using semi-continuous dilutions. The second set of cultures was not diluted further and was grown to the CO_2-limited stationary phase. These cultures allowed us to assess the effects of severe CO_2 limitation, in which growth was completely stopped. The same parameters listed above were measured at each sampling period in both sets of cultures. Supplemental nutrients and trace metals were added to the stationary phase cultures to ensure that growth was limited by low CO_2 (0.8–1.3 μmol L^{-1}) or associated high pH (8.89–9.01), rather than by nutrient limitation. The addition of supplemental nutrients caused no further increase in culture cell carbon or total cell volume, confirming that this was the case.

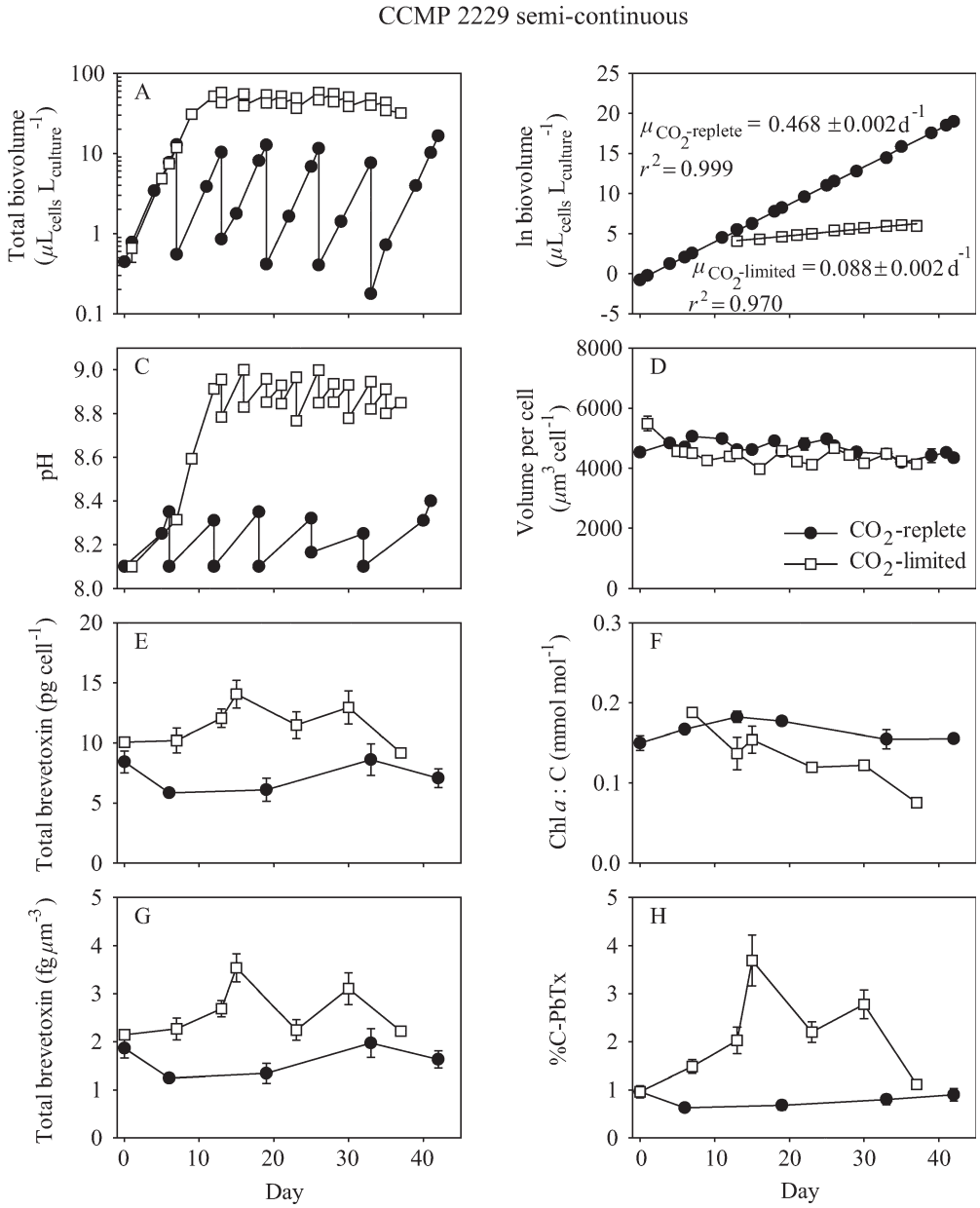

Fig. 2. Time-dependent results for semi-continuous batch culture of *Karenia brevis* strain CCMP 2229 grown under nutrient-sufficient CO_2-replete and CO_2-limited conditions: (A) growth curves of total culture biovolume ($\mu L_{cells} L_{culture}^{-1}$) vs. time (d), (B) curves for the natural log (ln) of total biovolume vs. time correcting for culture dilution (Sunda et al. 2007), (C) culture pH values vs. time (d), (D) mean volume per cell (μm^3 $cell^{-1}$), (E) total brevetoxins per cell (pg $cell^{-1}$), (F) Chl *a* normalized to cell carbon (mmol mol^{-1}), (G) brevetoxins normalized to cell volume (fg μm^{-3}), (H) brevetoxins as a percentage of cellular carbon (%C-PbTx). Error bars represent the standard deviation of three replicate measurements, except in panels F and H, where the cell carbon values were measured in duplicate.

Cell concentrations, mean volume, growth rate, Chl a*, cell C and N, and brevetoxins*—Aliquots for culture analyses were collected in the middle of the light period (midday). All analyses were conducted in triplicate, except for cellular carbon (C) and nitrogen (N), which were measured only in duplicate because of culture volume limitations. Results were expressed as mean values ± standard deviation unless otherwise noted.

Cell concentrations and mean volume per cell were measured with an electronic particle counter (Beckman Coulter Inc. Multisizer 3) equipped with a 100 μm, high-resolution aperture using a 0.5 mL sample volume. Cellular growth curves were constructed as semilog plots of total cell volume ($\mu L_{cells} L_{culture}^{-1}$) vs. time in days. Total cell volume ($\mu L_{cells} L_{culture}^{-1}$) was calculated by multiplying the cell concentration (cells L^{-1}) by the mean volume per cell

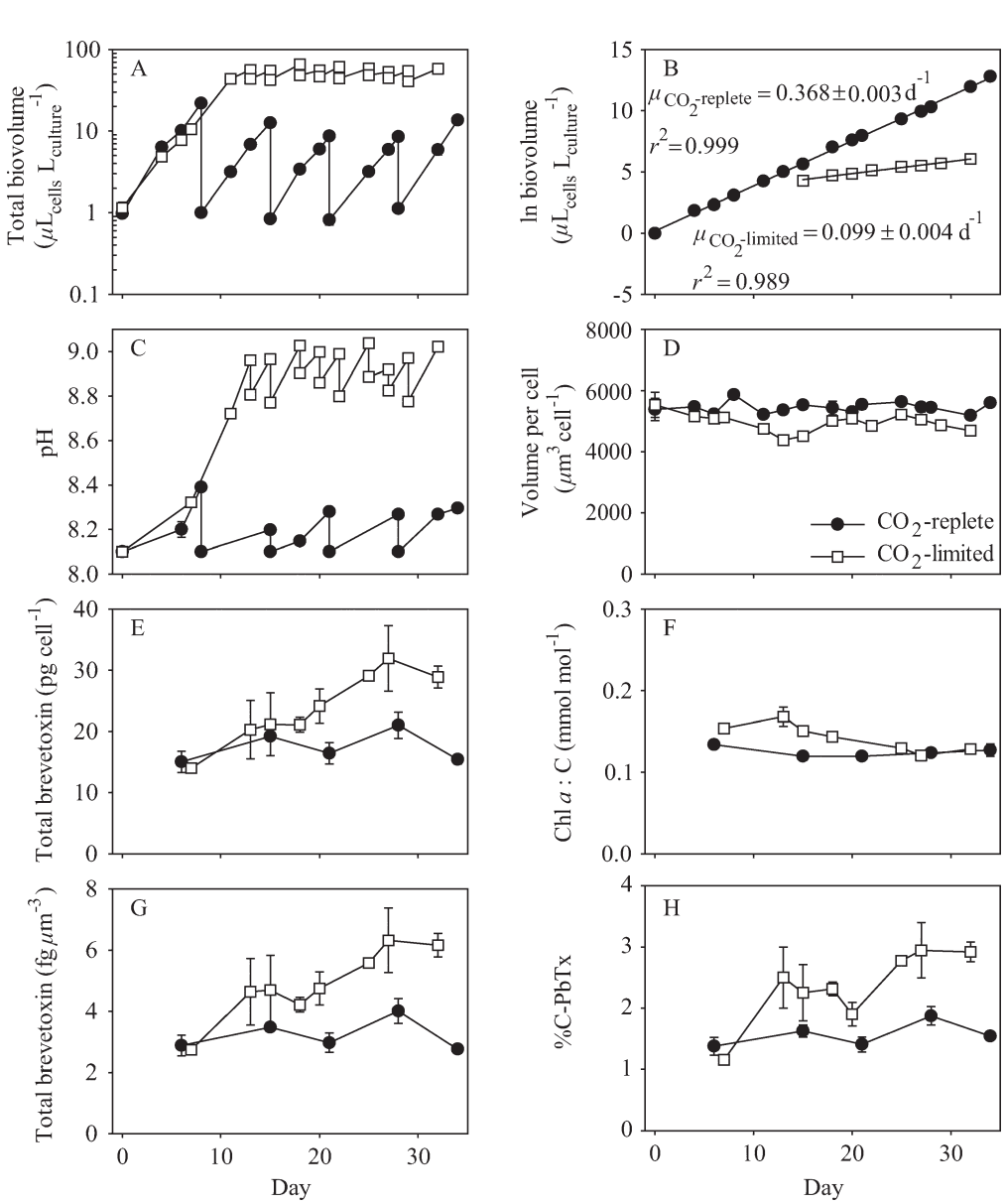

Fig. 3. Time-dependent results for semi-continuous batch culture of *Karenia brevis* strain SP3 grown under nutrient-sufficient CO_2-replete and CO_2-limited conditions: (A) growth curves of total culture biovolume ($\mu L_{cells} L_{culture}^{-1}$) vs. time (d), (B) curves for the natural log (ln) of total biovolume vs. time correcting for dilution (Sunda et al. 2007), (C) culture pH vs. time (d), (D) mean volume per cell (μm^3 $cell^{-1}$), (E) total brevetoxins per cell (pg $cell^{-1}$), (F) Chl *a* normalized to cell carbon (mmol mol^{-1}), (G) brevetoxins normalized to cell volume (fg μm^{-3}), (H) brevetoxins as a percentage of cellular carbon (%C-PbTx). Error bars represent the standard deviation of three replicate measurements, except in panels F and H, where the cell carbon values were measured in duplicate.

(μL $cell^{-1}$). Specific growth rates and associated standard errors were computed from linear regressions of the natural log of total cell volume vs. time after correcting for culture dilution (Sunda et al. 2007).

Chl *a* was determined by filtering cells onto 25 mm GF/F filters, extracting them with a 90% : 10% acetone : water mixture, and measuring the fluorescence of the extracted Chl *a* with a fluorometer (Turner Designs 10-AU; Welschmeyer 1994). Cellular C and N were determined by gentle filtration of cells onto precombusted 13 mm GF/F filters followed by fuming with HCl overnight to remove inorganic carbon. These filter samples were then analyzed for cellular N and C with an elemental analyzer (EAS 4010 Costech; Hardison et al. 2012).

Brevetoxins were analyzed by the same procedures as in previous N- and P-limitation experiments (Hardison et al. 2012, 2013). Brevetoxins were extracted from whole-culture aliquots using liquid–liquid separations with ethyl acetate. Before separation, aliquots of cell cultures were mixed 1 : 1 by volume with ethyl acetate, and the mixture was sonicated with a microtip-equipped sonicator (Qsonica, Q700) for 1 min. Complete cell disruption was confirmed

Table 1. Average values for specific growth rate, volume per cell, Chl *a*, total brevetoxins, brevetoxin biosynthetic rates, cell carbon to volume ratios, and molar N : C for CO_2-replete and CO_2-limited experiments with three strains of *Karenia brevis* (CCMP 2228, CCMP 2229, and SP3). Errors represent standard deviations (SDs) except for growth rates and brevetoxin biosynthetic rates, where standard errors (SEs) are given.

Treatment	Parameter	Unit	CCMP 2228	CCMP 2229	SP3
Semi-continuous culture experiments					
Nutrient-replete	Growth rate	d^{-1}	0.504±0.003	0.468±0.002	0.368±0.003
	Volume per cell	μm^3 $cell^{-1}$	4231±304	4654±239	5443±178
	Chl *a*	fg μm^{-3}	1.74±0.06	1.64±0.11	1.28±0.079
		mmol Chl *a* (mol C)$^{-1}$	0.196±0.029	0.164±0.013	0.125±0.006
	Total brevetoxin	fg μm^{-3}	2.73±0.29	1.61±0.32	3.22±0.52
		pg $cell^{-1}$	11.4±0.96	7.21±1.29	17.4±2.58
		% C-PbTx	1.93±0.42	0.96±0.14	1.57±0.2
	Brevetoxin biosynthetic rate	mmol C (mol C)$^{-1}$ d^{-1}	8.35±1.60	3.99±0.65	7.89±0.40
	C per cell volume	mol C L_{cells}^{-1}	8.30±1.50	9.42±1.26	11.4±0.81
	N : C	mol mol^{-1}	0.124±0.008	0.119±0.009	0.122±0.005
CO_2-limited	Growth rate	d^{-1}	0.091±0.006	0.088±0.002	0.099±0.004
	Volume per cell	μm^3 $cell^{-1}$	2858±287	4320±223	4949±301
	Chl *a*	fg μm^{-3}	0.880±0.137	0.880±0.050	1.39±0.11
		mmol Chl *a* (mol C)$^{-1}$	0.173±0.033	0.122±0.029	0.140±0.017
	Total brevetoxin	fg μm^{-3}	3.26±0.59	2.76±0.57	4.89±1.16
		pg $cell^{-1}$	9.36±2.38	11.9±1.83	23.8±5.89
		%C-PbTx	3.10±0.66	2.24±0.84	2.35±0.601
	Brevetoxin biosynthetic rate*	mmol C (mol C)$^{-1}$ d^{-1}	3.24±0.29 (d7–d15)	5.16±1.35 (d7–d15)	4.07±0.67 (d7–d13)
	C per cell volume	mol C L_{cells}^{-1}	6.78±1.54	7.72±1.87	11.4±0.73
	N : C	mol mol^{-1}	0.134±0.006	0.131±0.007	0.138±0.007
Batch culture experiments					
Nutrient-replete	Growth rate	d^{-1}	0.550±0.004	0.524±0.003	0.303±0.004
	Volume per cell	μm^3 $cell^{-1}$	3710±383	4441±201	5075±389
	Chl *a*	fg μm^{-3}	1.50±0.18	1.47±0.13	0.912±.077
		mmol Chl *a* (mol C)$^{-1}$	0.132±0.013	0.129±0.007	0.073±0.008
	Total brevetoxin	fg μm^{-3}	2.53±0.38	3.31±0.43	2.56±0.35
		pg $cell^{-1}$	8.84±1.44	14.9±2.05	12.2±1.77
		%C-PbTx	1.21±0.13	1.43±0.17	1.03±0.18
	Brevetoxin biosynthetic rate	mmol C (mol C)$^{-1}$ d^{-1}	6.65±0.35	7.51±0.34	3.13±0.27
	C per cell volume	mol C L_{cells}^{-1}	11.79±1.01	13.03±1.39	13.91±0.79
	N : C	mol mol^{-1}	0.117±0.005	0.109±0.012	0.114±0.009
CO_2-limited	Growth rate	d^{-1}	−0.001±0.002	0.020±0.002	0.017±0.009
	Volume per cell	μm^3 $cell^{-1}$	2350±146	2263±497	3568±320
	Chl *a*	fg μm^{-3}	0.689±0.201	0.572±0.239	1.06±0.073
		mmol Chl *a* (mol C)$^{-1}$	0.063±0.023	0.046±0.026	0.081±0.006
	Total brevetoxin	fg μm^{-3}	5.25±1.33	6.54±1.40	4.03±0.84
		pg $cell^{-1}$	12.2±2.75	14.74±3.24	14.2±2.32
		%C-PbTx	2.12±0.43	2.35±0.80	1.54±0.32
	Brevetoxin biosynthetic rate*	mmol C (mol C)$^{-1}$ d^{-1}	0.66±0.35 (d8–d23)	2.09±0.23 (d10–d22)	0.80±0.16 (d13–d23)
	C per cell volume	mol C L_{cells}^{-1}	12.79±1.57	14.63±3.84	11.4±0.73
	N : C	mol mol^{-1}	0.120±0.015	0.117±0.015	0.138±0.019

* For brevetoxin biosynthetic rates in the CO_2-limited cultures, the days of the experiment used for this calculation are given in parentheses.

by microscopy. The analysis gave total culture toxin concentration, which was deemed appropriate since preliminary experiments showed that > 90% of culture toxins were intracellular, corroborating previous findings (Tester et al. 2008; Lekan and Tomas 2010). Collected ethyl acetate fractions were desalted with Milli-Q™ water (18.2 MΩ) and concentrated with a rotovap (Büchi R-210). Extraction efficiency was determined in every fraction by the addition of a synthetic PbTx-3 methyl acetate internal standard (Lekan and Tomas 2010). Recovery efficiency typically ranged from 90% to 95%. Concentrated fractions were measured for brevetoxins using an Agilent 1100 liquid chromatograph (LC) coupled to a triple quadrupole mass spectrometer (MS, Thermo-Finnigan TSQ Quantum, Thermo Fisher Scientific) with an electrospray ion source interface. LC-MS-MS conditions have been previously

Table 2. Average pH and corresponding calculated CO_2 concentrations (μmol L^{-1}) for the three *Karenia brevis* strains growing at their maximum rates (Table 1) in nutrient- and CO_2-sufficient semi-continuous cultures compared with values for cultures growing at a reduced rate (μ = ~0.1 d^{-1}) in semi-continuous cultures at low CO_2 and high pH and under stationary phase growth (μ = 0) in batch cultures. The CO_2 values ± standard deviation (SD) were calculated from measured pH values (National Bureau of Standards scale) and the seawater alkalinity using the computer program CO2SYS as described in Methods.

	Semi-continuous culture experiments				Batch culture experiments			
	CO_2-replete		CO_2-limited, μ = 0.1 d^{-1}		CO_2-replete		CO_2-limited, μ = 0.0 d^{-1}	
Strain	CO_2 (μmol L^{-1})	pH	CO_2 (μmol L^{-1})	pH	CO_2 (μmol L^{-1})	pH	CO_2 (μmol L^{-1})	pH
CCMP 2228	11.0±3.4	8.22±0.13	1.28±0.40	8.89±0.08	12.0±3.3	8.19±0.12	1.00±0.28	8.96±0.08
CCMP 2229	10.7±3.4	8.23±0.11	1.28±0.33	8.89±0.07	8.5±4.1	8.31±0.19	1.25±0.53	8.90±0.10
SP3	11.6±3.0	8.20±0.09	1.21±0.41	8.91±0.09	11.0±2.6	8.22±0.08	0.83±0.28	9.01±0.06

described in detail (Cheng et al. 2005; Mendoza et al. 2008). An external standard curve of purified brevetoxins 1, 2, and 3 (World Ocean Solutions) was used to quantify amounts of extracted brevetoxins.

Calculations—All CO_2-limited values presented in Tables 1 and 2 were means of measurements taken after growth limitation occurred, typically by days 10–15 of the experiment, depending on strain tested (Figs. 1–6, panels B).

Net biosynthetic rates of brevetoxins (V_B) were computed for both the control and the CO_2-limited cultures using the equation

$$\frac{dQ}{dt} = V_B - \mu Q \quad (1)$$

where Q is the carbon-normalized cellular brevetoxin concentration, dQ/dt is the change in cellular brevetoxin (Q) with time, and μ is the specific growth rate. In exponentially growing cultures at steady state, the cellular brevetoxin levels should be constant ($dQ/dt \sim 0$). Thus, under these conditions, Eq. 1 collapses to:

$$V_B = \mu Q \quad (2)$$

This equation was used to compute V_B values for the CO_2-sufficient control cultures. Net biosynthetic rates (V_B) for the CO_2-limited cultures in which dQ/dt was positive were computed from a rearrangement of Eq. 1,

$$V_B = \frac{dQ}{dt} + \mu Q \quad (3)$$

where dQ/dt is the average rate of increase in Q and μQ is the specific growth rate times the average value of Q over the time interval in question. For the stationary phase of the CO_2-limited batch cultures, $\mu = 0$ and the mean biosynthetic rate simply equals the average rate of increase in Q with time. The average rates of increase (dQ/dt) in Eq. 3 were determined from linear regressions of Q vs. time.

Equilibrium calculations were used to compute various components of the CO_2 system in our culture media. Concentrations of CO_2 in the culture media were calculated from the measured pH and the computed alkalinity using the CO2SYS computer program (Sunda and Cai 2012). The initial culture alkalinity of our Gulf Stream water–based medium (2.35 mmol kg^{-1}) was computed from the published relationship between total alkalinity and salinity for surface North Atlantic seawater (Lee et al. 2006). The salinity of the Gulf Stream seawater (36) was measured with a salinometer (ThermoOrion, 135A, Thermo Scientific). During culture growth, alkalinity increases slightly because of the assimilation of nitrate into cellular organic N, which increases alkalinity by 1 mol kg^{-1} for each mol kg^{-1} of nitrate assimilated (Sunda and Cai 2012). In high-density, CO_2-limited cultures, the alkalinity was computed to equal the initial value plus that added by nitrate assimilation into cell N. Measured cellular N concentrations ranged from 39.4 ± 3.3 μmol kg^{-1} of medium for CO_2-limited, semi-continuous cultures of strain CCMP 2228 to an average maximum value of 97.2 ± 3.3 μmol kg^{-1} during the stationary phase of CO_2-limited batch cultures of strain SP3. These nitrate assimilation values caused only small computed increases in alkalinity equaling 1.7% to 4.1%.

A model was also constructed to calculate the changes in total inorganic carbon (TIC) in seawater due to CO_2 fixation in CO_2-limited algal blooms at atmospheric partial pressures of CO_2 (P_{CO_2}) of 28, 41, and 81 Pa (equivalent to 280, 400, and 800 ppm), representing preindustrial, current, and year 2100 values. To do this we first computed the initial prebloom TIC values for surface North Atlantic seawater at our experimental temperature (23°C), salinity (36), and associated total alkalinity (2.35 mmol kg^{-1}) at P_{CO_2} values of 28, 41, and 81 Pa. We then computed the TIC of seawater at the mean pH value (9.0) at which our *K. brevis* strains stopped growing because of CO_2 limitation. The difference in these two TIC values provided an estimate of the algal carbon biomass (mol C kg^{-1} of seawater). These calculations were performed with the computer program CO2SYS (Sunda and Cai 2012). In these calculations the alkalinity at high-bloom carbon values was adjusted upward slightly to account for nitrate assimilation by the algae. As described previously, this increase equaled the concentration of nitrogen assimilated by the algae, which was calculated from the computed concentration of fixed carbon and the average measured C : N in the CO_2-limited *K. brevis* cultures at pH 9.0.

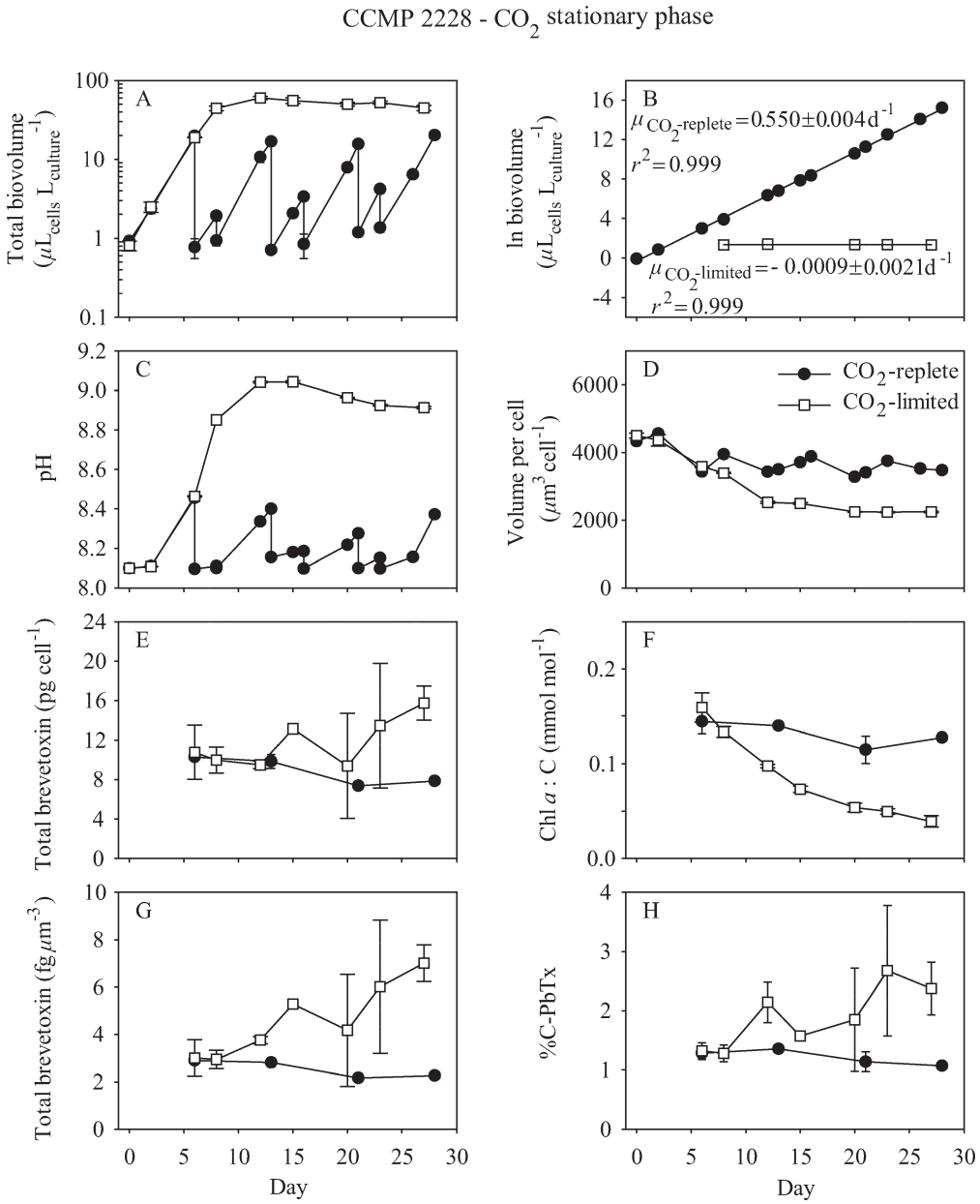

Fig. 4. Time-dependent results for semi-continuous batch cultures of the CO_2-replete *Karenia brevis* strain CCMP 2228 and a batch culture of this strain that was allowed to grow into CO_2 limitation in stationary phase: (A) growth curves of total culture biovolume ($\mu L_{cells} L_{culture}^{-1}$) vs. time (d), (B) curves for the natural log (ln) of total cell volume vs. time correcting for culture dilution (Sunda et al. 2007), (C) culture pH vs. time, (D) mean volume per cell (μm^3 $cell^{-1}$), (E) total brevetoxins per cell (pg $cell^{-1}$), (F) Chl *a* normalized to cell carbon (mmol mol^{-1}), (G) brevetoxins normalized to cell volume (fg μm^{-3}), (H) brevetoxins as a percentage of cellular carbon (%C-PbTx). Error bars represent the standard deviation of three replicate measurements, except in panels F and H, where the cell carbon values were measured in duplicate.

Results

The maximum growth rates in the CO_2-replete *K. brevis* cultures varied from 0.30 d^{-1} for strain SP3 to 0.55 d^{-1} for strain CCMP 2228 (Table 1; Figs. 1–6, panels B). The corresponding mean cell volumes varied from 3710 μm^3 for CCMP 2228, the fastest growing strain, to 5443 μm^3 for SP3, the slowest growing strain (Table 1, Figs. 1–6, panels D). Average CO_2 concentrations in the CO_2-replete, exponentially growing cultures ranged from 8.5 to 12.0 μmol L^{-1} (Table 2). Average CO_2 levels in the CO_2-limited cultures growing at a specific rate of 0.1 d^{-1} were substantially lower (1.2–1.3 μmol L^{-1}; Table 2). The CO_2 concentrations in the stationary phase batch cultures ranged from 0.8 μmol L^{-1} (SP3) to 1.3 μmol L^{-1} (CCMP 2229).

Cell size, Chl a*, and N : C*—As CO_2 concentrations declined, the cells were expected to decrease in size to increase their surface to volume ratios and the diffusive flux of CO_2

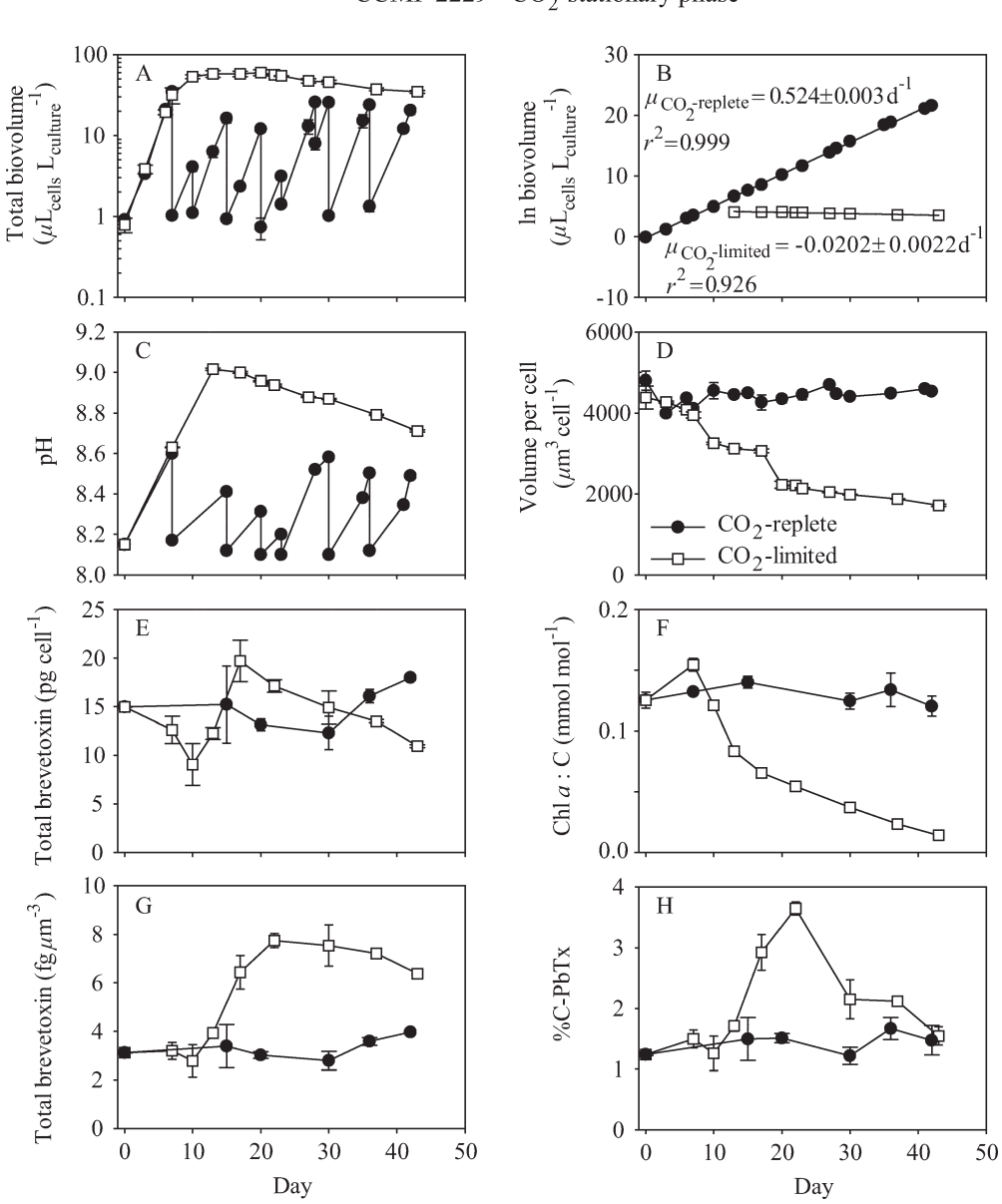

Fig. 5. Time-dependent results for semi-continuous batch cultures of the CO_2-replete *Karenia brevis* strain CCMP 2229 and a batch culture of this strain that was allowed to grow into CO_2 limitation in stationary phase: (A) growth curves of total culture biovolume ($\mu L_{cells} L^{-1}_{culture}$) vs. time (d), (B) curves for the natural log (ln) of total biovolume vs. time correcting for culture dilution (Sunda et al. 2007), (C) measured culture pH vs. time, (D) mean volume per cell (μm^3 cell^{-1}), (E) total brevetoxins per cell (pg cell^{-1}), (F) Chl *a* normalized to cell carbon (mmol mol^{-1}), (G) brevetoxins normalized to cell volume (fg μm^{-3}), (H) brevetoxins as a percentage of cellular carbon (%C-PbTx). Error bars represent the standard deviation of three replicate measurements, except in panels F and H, where the cell carbon values were measured in duplicate.

through the cell's surface boundary layer (Sunda and Hardison 2010). All three strains followed this expected pattern, but the decrease in cell size varied among strains and between the two sets of CO_2-limitation experiments. Strain CCMP 2228 showed similar decreases in mean volume per cell (32% and 37%, respectively) in the CO_2-limited semi-continuous cultures and stationary phase batch cultures relative to values in the CO_2-sufficient controls (Table 1; Figs. 1A, 4A). The other two strains showed large differences between the semi-continuous and batch culture experiments. The mean volume per cell in the CO_2-limited semi-continuous cultures of strains CCMP 2229 and SP3 were 7% and 9% lower, respectively, than that of the CO_2-sufficient controls (Table 1;

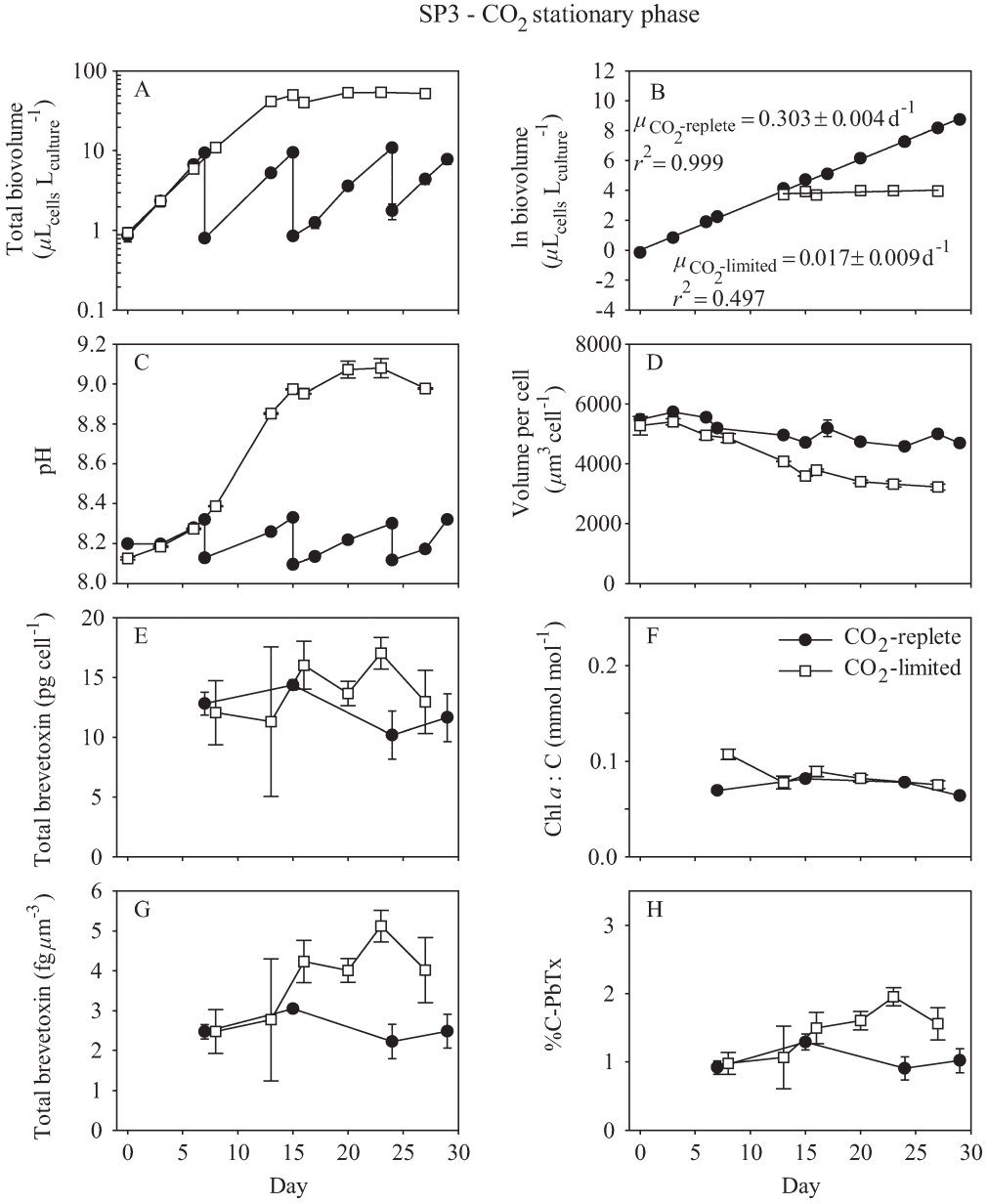

Fig. 6. Time-dependent results for semi-continuous batch cultures of the CO_2-replete *Karenia brevis* strain SP3 and a batch culture of this strain that was allowed to grow into CO_2 limitation in stationary phase: (A) growth curves of total culture biovolume ($\mu L_{cells} L_{culture}^{-1}$) vs. time (d), (B) curves for the natural log (ln) of total biovolume vs. time correcting for culture dilution (Sunda et al. 2007), (C) culture pH vs. time, (D) mean volume per cell (μm^3 $cell^{-1}$), (E) total brevetoxins per cell (pg $cell^{-1}$), (F) Chl *a* normalized to cell carbon (mmol mol^{-1}), (G) brevetoxins normalized to cell volume (fg μm^{-3}), (H) brevetoxins as a percentage of cellular carbon (%C-PbTx). Error bars represent the standard deviation of three replicate measurements, except in panels F and H, where the cell carbon values were measured in duplicate.

Figs. 2A, 3A). By contrast, cell volume declined by 49% and 30%, respectively, relative to control values during stationary phase in the batch culture experiment (Table 1; Figs. 5A, 6A).

Previous studies on N and P limitation of growth rate in *K. brevis* showed that as growth slowed, Chl *a* was consistently down-regulated to bring carbon fixation into balance with growth (Hardison et al. 2012, 2013). In the present study, a decrease was also observed in Chl *a* : cell volume with the onset of growth rate limitation (at approximately days 12–13) in the semi-continuous cultures of the two faster growing strains CCMP 2228 and CCMP 2229 ($p < 0.001$; Tables 1, 3). On average in these strains, Chl *a* per unit of cell volume decreased by 46–50% in the CO_2-limited semi-continuous cultures relative to control culture values, and by 54–61% in the stationary phase batch cultures that had ceased growing (Table 1). By contrast, Chl *a* : cell volume in the CO_2-limited semi-continuous cultures and stationary phase batch cultures of strain SP3 were 9% and 16% higher, respectively, than

Table 3. Statistical significance (p values) of differences in mean volume per cell, Chl a (normalized to cell volume and cell carbon), cellular brevetoxins (normalized per cell, per unit of cell volume, and as a percentage of cell carbon), and cell N : C between nutrient-replete control, CO_2-sufficent cultures, and either CO_2-limited semi-continuous cultures ($\mu = 0.1\ d^{-1}$) or stationary phase batch cultures ($\mu = 0\ d^{-1}$). Statistical significance was determined at the 0.05 level by t-test for normal distributions and by Mann–Whitney U-test for nonnormal distributions.

	CCMP 2228				CCMP 2229				SP3			
	Test	Stat	df	p	Test	Stat	df	p	Test	Stat	df	p
Semi-continuous culture experiments												
Volume per cell (μm^3)	t	9.06	15	<0.001	t	3.74	27	<0.001	t	5.41	27	<0.001
Chl a (fg μm^{-3})	t	12.8	7	<0.001	t	15.0	8	<0.001	U	5.00	—	0.030
Chl a : C (mmol mol^{-1})	t	1.52	9	0.163	t	3.23	9	0.100	t	−1.85	9	0.097
PbTx (fg μm^{-3})	t	−2.94	7	0.026	t	−3.96	8	0.004	t	−3.01	11	0.012
PbTx (pg $cell^{-1}$)	U	3.00	—	0.111	t	−4.74	8	0.001	t	−2.27	11	0.044
%C-PbTx	t	−1.42	7	0.004	t	−3.64	8	0.007	t	−2.77	11	0.018
N : C (mol mol^{-1})	U	41.0	—	<0.001	U	4.00	—	<0.001	U	13.0	—	<0.001
Stationary phase batch culture experiments												
Volume per cell (μm^3)	U	8.00	—	0.003	U	1.00	—	<0.001	t	8.07	15	<0.001
Chl a (fg μm^{-3})	t	5.67	6	0.001	t	8.57	11	<0.001	U	2.00	—	0.063
Chl a : C (mmol mol^{-1})	t	5.27	7	0.001	U	0.00	—	0.002	t	−1.77	7	0.120
PbTx (fg μm^{-3})	U	0.00	—	0.016	U	1.00	—	0.004	t	−3.26	7	0.014
PbTx (pg $cell^{-1}$)	t	−2.22	7	0.062	t	0.14	10	0.893	t	−1.38	7	0.211
%C-PbTx	U	0.00	—	0.016	t	−2.78	10	0.020	t	−2.81	7	0.026
N : C (mol mol^{-1})	U	36.0	—	0.183	t	−2.81	26	0.026	U	14.0	—	0.020

observed in the CO_2-sufficient control cultures, suggesting an up-regulation of the photosynthetic apparatus (Tables 1, 3). The observed increase was statistically significant for the CO_2-limited semi-continuous culture and just missed being significant for the stationary phase batch culture (Table 3). Similar trends were seen when Chl a was normalized to cell carbon (mmol Chl a [mol C]$^{-1}$); however, the magnitudes of the changes were different due to variations in C : cell volume (Table 1; Figs. 1–6, panels F). In strains CCMP 2228 and CCMP 2229, Chl a : C decreased on average by 12–26% in the CO_2-limited semi-continuous cultures relative to control values (Table 1; Figs. 1F, 2F) and decreased by 52–64% during stationary phase in the batch cultures relative to controls (Table 1; Figs. 4F, 5F). Chl a : C in strain SP3 increased on average by 12% in the CO_2-limited semi-continuous cultures and by 11% in the stationary phase batch culture compared with control values (Table 1; Figs. 3F, 6F), but the increases were not statistically significant (Table 3).

Chl a : C values were plotted as a function of specific growth rate for CO_2-limited cultures in the present study and for P-limited cultures of strains CCMP 2228 and CCMP 2229 from a previous study (Hardison et al. 2013; Fig. 7A). These data show a larger down regulation in Chl a : C in P-limited cultures than in CO_2-limited cultures, as growth rate declined from maximum values to $\sim 0.1\ d^{-1}$. The decrease in Chl a : C in the P-limited cultures was 41–51% in strains CCMP 2228 and CCMP 2229 compared with the 12–26% decreases noted above under equivalent CO_2 limitation for these same two strains (Fig. 7A). A t-test of the slopes of Chl a : C vs. specific growth rate, however, showed that the larger decrease in Chl a : C in the P-limited cells was significant only for strain CCMP 2229 (t-test, $t = -2.32$, degrees of freedom [df] = 17, $p = 0.033$), but not for strain CCMP 2228 (t-test, $t = -1.74$, df = 24, $p = 0.095$).

Strain SP3 was not examined in our previous experiments investigating the effects of P limitation on cellular Chl a (Hardison et al. 2013); however, it was examined in a parallel N-limitation experiment, where only Chl a : cell volume was measured, but not Chl a : cell C (Hardison et al. 2012). In that experiment, N limitation of growth rate to a value of $0.1\ d^{-1}$ caused a 48% decrease in the Chl a : cell volume in strain SP3. By contrast, the same decrease in SP3 growth rate to $0.1\ d^{-1}$ under CO_2 limitation resulted in a 9% increase in the Chl a : cell volume ($p = 0.030$; Tables 1, 3).

Marked differences in cellular response to CO_2 limitation and P limitation were also seen for cellular N : C. These ratios were 8–13% higher in CO_2-limited cultures growing at a specific rate of $0.1\ d^{-1}$ than ratios observed in the CO_2-sufficient control cultures ($p \leq 0.001$; Tables 1, 3; Fig. 7B). By comparison, in a previous study (Hardison et al. 2012), cellular N : C values in P-limited cultures of strains CCMP 2228 and CCMP 2229 growing at the same low specific rate ($0.1\ d^{-1}$) were 20–21% lower than values in the control cultures (CCMP 2228: t-test, $t = 7.31$, df = 16, $p \leq 0.001$; CCMP 2229: t-test, $t = 0.025$, df = 11, $p \leq 0.001$; Fig. 7B).

The above results indicate that growth limitation by low CO_2 (or accompanying high pH) results in both higher cellular N : C and Chl a : C (or Chl a : cell volume) than observed under equivalent growth rate limitation by N or P in previous studies (Hardison et al. 2012, 2013). This effect was greatest in clone SP3, where cellular Chl a : cell volume and Chl a : C actually increased with CO_2 limitation of growth rate. Additionally, the Chl a : C and N : C values were higher in strain SP3 than in the other two strains in the stationary phase batch cultures (Table 1; Fig. 7B).

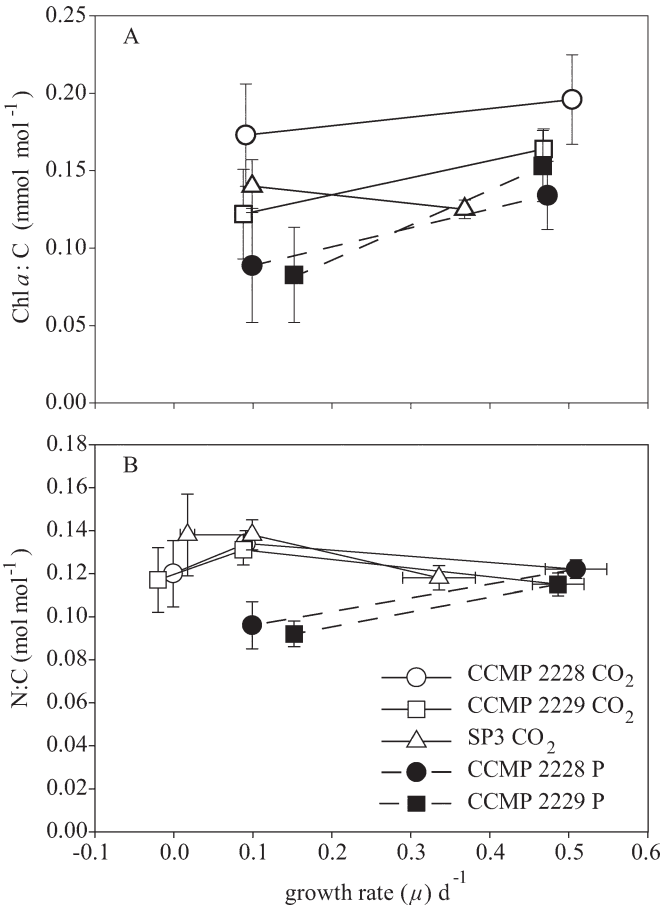

Fig. 7. Average values for (A) Chl *a* normalized to cell C (mmol Chl *a* [mol C]$^{-1}$) plotted vs. specific growth rate (μ) and (B) for cellular N : C (mol mol^{-1}) plotted vs. specific growth rate in three *Karenia brevis* strains. The data from CO_2-limited cultures in this study are indicated by open circles (CCMP 2228), open squares (CCMP 2229), and open triangles (SP3) joined by solid lines. Data from a previous study in which the growth rate of *K. brevis* was limited by phosphorus (Hardison et al. 2013) are indicated by closed circles (CCMP 2228) and squares (CCMP 2229) joined by dashed lines. (A) Data only for semi-continuous culture experiments. (B) Data from both semi-continuous and batch culture experiments. The maximum CO_2- and nutrient-sufficient growth rates and associated N : C in panel B are combined means from the control culture data for both the semi-continuous and batch culture experiments (Figs. 1–6, panels B; Table 1).

Brevetoxins—Cellular brevetoxins increased with CO_2 limitation of growth rate in the semi-continuous cultures and stationary phase of the batch cultures, but the amount and pattern of increase was dependent on whether the brevetoxins were normalized to cell carbon, cell volume, or per cell (Figs. 1–6, panels E, G, H). Brevetoxins expressed as a percentage of cell carbon (%C-PbTx) provides a direct measure of the fraction of cellular carbon present in PbTxs. Brevetoxin per unit of cell volume (fg μm^{-3}), on the other hand, provides an integrated measure of changes in %C-PbTx and cell C : volume. The brevetoxin per cell response is the most complex in that it is governed by simultaneous changes in %C-PbTx, the cell C : volume, and mean volume per cell, all of which change to varying degrees with CO_2 limitation of growth rate (Table 1).

Of the three cell normalizations, %C-PbTx provides the best measure of the amount of brevetoxins per unit of cellular organic matter. The %C-PbTx began to increase in the low dilution (0.1 d^{-1}) semi-continuous cultures and stationary phase batch cultures on about day 10 as CO_2 began to limit algal growth (Figs. 1–6, panels H). Thereafter, two different patterns were observed depending on the strain and the CO_2-limitation treatment. In CO_2-limited semi-continuous cultures of strains CCMP 2228 and 2229 and the stationary phase culture of strain CCMP 2229, the %C-PbTx values first increased to a maximum and then declined to levels slightly higher than those observed in the CO_2-sufficient cultures (Figs. 1H, 2H, 5H). However, in the CO_2-limited semi-continuous culture of strain SP3 and the stationary phase cultures of strains CCMP 2228 and SP3, the %C-PbTx values rose and then plateaued (Figs. 3H, 4H, 6H). Hence, the %C-PbTx response pattern for strains CCMP 2229 and SP3 remained similar in both the CO_2-limited semi-continuous cultures and stationary phase cultures. Strain CCMP 2228, by contrast, shifted from a rise and fall pattern in the CO_2-limited, semi-continuous culture to a rise and plateau pattern in the stationary phase culture (Figs. 1H, 4H).

The maximum %C-PbTx with CO_2 limitation of growth rate was generally higher in the semi-continuous cultures than in the stationary phase of the batch cultures. In strain CCMP 2228, %C-PbTx increased to a maximum of 2.8% in the stationary phase of the batch culture compared with a maximum of 3.8% in the CO_2-limited semi-continuous culture. In strain SP3 the maximum %C-PbTx was also lower in the stationary phase batch culture (2.0%) than in the CO_2-limited semi-continuous batch culture (2.8%). However, in strain CCMP 2229 the maximum %C-PbTx in both of the CO_2-limited cultures was the same (3.7%).

Brevetoxin per unit of cell volume showed similar patterns of increase to those observed for %C-PbTx because the cell C to volume ratios showed only small changes ranging from an 18% decrease in CO_2-limited semi-continuous cultures of strains CCMP 2228 and 2229 to slight increases of 8–12% in CO_2-limited stationary phase cultures of these same two strains (Table 1; Figs. 1–6, panels G, H). The differences in response patterns were greater for brevetoxins per cell (Fig. 1–6, panels E, G, H) because, in addition to the changes in cell C to volume ratios, there were 9–32% decreases in mean volume per cell in the CO_2-limited semi-continuous cultures and 30–49% decreases in this same parameter in the CO_2-limited stationary phase cultures (Table 1). Because of these decreases in volume per cell, the increases in average brevetoxin per cell were smaller (0.82–1.38-fold) than those observed for %C-PbTx (1.49–2.33-fold) or brevetoxin per unit cell volume (1.19–2.08-fold) (Table 1).

The increases in mean %C-PbTx and cellular brevetoxin per unit of cell volume under CO_2 limitation in our three experimental strains were statistically significant in both the semi-continuous and the batch culture experiments ($p \leq 0.026$; Table 3). These increases were compared with those observed under equivalent growth rate limitation in our

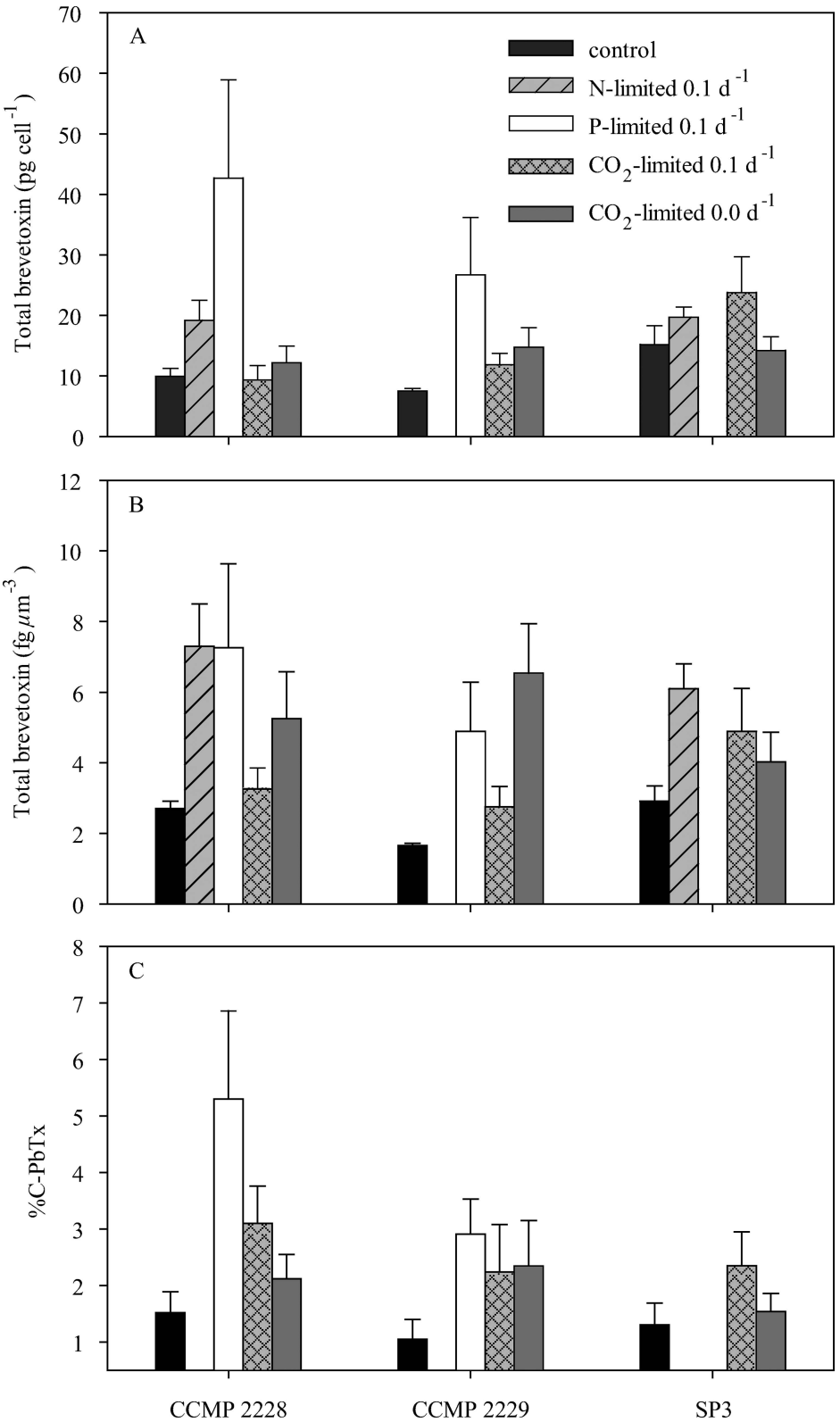

Fig. 8. A comparison of the toxin response of three strains of *Karenia brevis* collated from four separate nutrient- and CO_2-limited growth studies: (A) total brevetoxins per cell (pg cell^{-1}), (B) brevetoxins normalized to cell volume (fg μm^{-3}), and (C) brevetoxins as a percentage of total cellular carbon (%C-PbTx). Control values across all three limitations were averaged together and are represented by the black bars. The N-limited (diagonal hatch and grey), P-limited (white), CO_2-limited (μ = 0.1 d^{-1}; cross hatch and grey), and CO_2-limited stationary phase (grey) values were calculated by averaging values after the reduction of growth rate occurred after approximately day 10 in each of the studies.

previous N- and P-limitation experiments with these same strains (Hardison et al. 2012, 2013; Fig. 8). All strains increased in toxicity as growth slowed, but the toxin increases under CO_2 limitation were less than those under equivalent N or P limitation of growth rate. Toxins per unit of cell volume (fg μm^{-3}) were 25–50% lower under CO_2 limitation than for similar decreased growth rate under N and P limitation ($p = 0.003$–0.024, t-test; Fig. 8B). Toxins as a percentage of cell carbon were also lower under CO_2 limitation than under P limitation (Fig. 8C). Here, the %C-PbTx was 46% lower in CO_2-limited cells than in P-limited cells for strain CCMP 2228 (t-test, $t = 3.32$, df = 7, $p = 0.013$) and 27% lower in strain CCMP 2229, although this latter difference was not statistically significant (t-test, $t = 1.46$, df = 11, $p = 0.17$). A similar %C-PbTx comparison cannot be made with previous N-limitation experiments for strain SP3 because of a lack of cell carbon data in those experiments (Fig. 8C); however, as noted above, the PbTx to cell volume ratio in the CO_2-limited culture of this strain was significantly less than that observed in the N-limited culture (t-test, $t = 2.55$, df = 13, $p = 0.024$). The patterns observed for toxin per cell were somewhat different (Fig. 8A) because of differing changes in mean volume per cell under N, P, and CO_2 limitation.

Figure 8 also shows a comparison of cellular brevetoxins among semi-continuous control cultures, CO_2-limited semi-continuous cultures ($\mu = 0.1\ d^{-1}$), and CO_2-limited batch cultures that had ceased growing. In strain CCMP 2229, the %C-PbTx values were the same in the CO_2-limited semi-continuous culture and the CO_2-limited stationary phase batch culture. However, %C-PbTx values were 32–34% lower in the CO_2-limited stationary phase batch cultures of strains CCMP 2228 and SP3 relative to values in the CO_2-limited semi-continuous cultures of these strains. This latter pattern was similar to that noted above for maximum %C-PbTx values.

Discussion

Comparison with predictions of the CNB hypothesis—This study documented the effect of CO_2 limitation of growth rate on cellular brevetoxins in *K. brevis* to determine whether the cellular response conforms to the CNB hypothesis. The CNB hypothesis states that as plant growth slows under nutrient limitation, an imbalance occurs between carbon fixation and the supply of the limiting nutrients (Bryant et al. 1983). Under these conditions plants (including algae) divert some of the excess fixed carbon into C-based defensive compounds, such as toxins, to help alleviate this imbalance. This diversion serves two important functions: it protects the photosynthetic apparatus from overreduction and resulting oxidative stress (Niyogi 1999) until a balance between photosynthesis and growth can be achieved, and it decreases specific rates of grazing mortality (Hong et al. 2012; Waggett et al. 2012) to bring them more into line with the lower nutrient-limited specific rates of cellular growth and reproduction. Studies of N and P limitation of *K. brevis* have shown that, depending on the isolate, the percentage of the cell carbon pool invested in brevetoxins increases from 0.8% to 2.1% under nutrient sufficiency to 1.6–5.3% under growth limitation in accordance with predictions of the CNB hypothesis (Hardison et al. 2012, 2013). Even though brevetoxins occur at a relatively low percentage of cell carbon, they still represent a significant investment of resources in a single related group of defensive compounds. Typically, the various secondary metabolites used for chemical defenses in marine macroalgae constitute 0.2–2% of the carbon pool, but they can be as high as 15% in some cases (Hay and Fenical 1988).

In contrast to nutrient limitation, in CO_2 limitation of *K. brevis* there is no excess fixed carbon to divert into toxins. Here, the CNB hypothesis predicts that the concentration of carbon-based antigrazing toxins, such as brevetoxins, should remain the same or decrease. Our results, however, are contrary to the predictions of this hypothesis, in that toxin concentrations increased as growth rates slowed under CO_2 limitation (Figs. 1–3, panels H).

This toxin increase clearly showed that even though there is no "excess" fixed carbon to divert into C-based toxins under CO_2 limitation, *K. brevis* cells still invested a greater percentage of their fixed carbon pool into PbTxs than did CO_2-replete cells. This observation is consistent with a strong evolutionary selection for increasing cellular C-based toxins as growth slows, even under severe CO_2 limitation of C fixation and growth. However, the restricted supply of fixed carbon under CO_2 limitation of growth rate generally results in smaller increases in brevetoxins than observed under equivalent N- or P-limited growth rates (Fig. 8). Thus, CO_2 limitation does constrain how much C can be invested in PbTxs relative to that invested under N or P limitation, where excess carbon becomes "available" as growth slows.

Cellular brevetoxin levels are determined by the relative balance between net cellular biosynthetic rates and biodilution by growth (*see* Eqs. 1, 2 in Methods). An analysis of our data indicate that the increase in %C-PbTx values in the initial stages of CO_2 limitation in both the semi-continuous and batch culture experiments was not due to an increase in specific rates of brevetoxin biosynthesis, as these rates remained the same or decreased in all cases but one (Table 1). The sole exception was the CO_2-limited semi-continuous culture of strain CCMP 2229 where the CO_2-limited biosynthetic rate increased by 29% (Table 1); however, this increase was not significant (t-test, $t = 0.78$, df = 5, $p = 0.24$). Instead of an increase in biosynthetic rates, the increase in cellular brevetoxins in the CO_2-limited cultures was caused in most cases by the large decline in specific growth rate, which decreased to a larger degree than the decrease in the biosynthetic rates of brevetoxins (Table 1). Thus, although there is a decrease in brevetoxin biosynthetic rates in the CO_2-limited cells, there is an even larger decrease in the biosynthetic rates of other critical cellular constituents, such as proteins, carbohydrates, and lipids. This relative downward shift in rates results in a larger fraction of the cellular carbon pool being invested in brevetoxins.

Other studies have also shown a similar increase in cellular toxins or cell toxicity as growth rate slows at low CO_2 concentrations and associated high pH. Elevated pH

and low CO_2 increased the toxicity of *Prymnesium parvum* to fish (Ulitzur and Shilo 1964, 1966) and increased the toxic effect of another prymnesiophyte, *Chrysochromulina polylepis*, on co-occurring phytoplankton (Schmidt and Hansen 2001). Likewise, a decrease in growth rate at low CO_2 and high pH caused a substantial increase in the cell content of the neurotoxin domoic acid in the diatoms *Pseudo-nitzschia multiseries* and *Nitzschia navis-varingica* (Lundholm et al. 2004; Trimborn et al. 2008). As in our present experiments, the increase in cell toxicity in these studies occurred at pH values > 8.6 ($CO_2 < 4.3$ μmol L^{-1}). Somewhat different results were observed in experiments with *P. multiseries* and *Pseudo-nitzschia fraudulenta* when the P_{CO_2} of culture media was raised from a preindustrial value of 22 Pa (pH 8.4) to a value projected to occur near the end of the current century, 74 Pa (pH 7.9). In these experiments, the CO_2 increase caused a three- to fourfold increase in domoic acid per cell, but this effect only occurred in cells whose growth rate was reduced by phosphate or silicate limitation, which by themselves caused 7- to 50-fold increases in domoic acid per cell (Sun et al. 2011; Tatters et al. 2012). Thus, while growth limitation by nutrients (phosphate and silicate) and CO_2 by themselves can increase cellular toxin levels, nutrient limitation at high future CO_2 levels may cause combined results quite different from the additive effects of the two stressors alone.

Carbon-concentrating mechanisms and CO_2 limitation—Because of the low CO_2 binding affinity of the carbon-fixing enzyme ribulose-1,5-bisphosphate carboxylase oxygenase (RuBisCO), most phytoplankton employ carbon concentrating mechanisms (CCMs) to pump CO_2 into the cell (Falkowski and Raven 2007). CCMs have been identified in bloom-forming dinoflagellates and are up-regulated at low external CO_2 concentrations (Giordano et al. 2005; Rost et al. 2006). Previous studies have shown that the growth rate of various phytoplankton species is limited by CO_2 over a wide pH range (8.3–10) and associated large range of CO_2 concentrations (Hansen 2002). This large range of growth-limiting CO_2 values was attributed to variations in the ability of different species to concentrate CO_2 intracellularly via CCMs at low external CO_2. The data from our study suggests that *K. brevis* has a relatively efficient CCM because it is able to grow optimally at CO_2 concentrations down to 2.4 μmol L^{-1} (pH 8.7), and growth rate ceases at CO_2 levels of ~ 1 μmol L^{-1} (pH 9.0; Figs. 4–6, panels C; Table 2). A similar ability to grow at low CO_2 (high pH) is observed in the toxic dinoflagellate *Karenia mikimotoi,* which co-occurs with *K. brevis* in Florida red tide blooms and also forms extensive high-density blooms in coastal waters of Europe and Asia (Brand et al. 2012). The growth of this species is limited by CO_2 at pH > 8.7, and growth ceased at pH 9.0 (Hansen 2002), the same as observed in *K. brevis*. The ability of these toxic dinoflagellates to grow at low CO_2 concentrations and associated high pH likely contributes to their ability to form high biomass blooms.

The exact nature of the CCM is not known in most cases, including in *K. brevis* (Giordano et al. 2005). However, it is well documented that CCMs are fueled either directly or indirectly by photosynthetically produced adenosine-5′-triphosphate (ATP; Giordano et al. 2005). Our results showed that as N- and P-sufficient cells grew into CO_2 limitation, their Chl *a* : C or Chl *a* : cell volume ratios were higher than those observed at similar specific growth rates under P or N limitation of growth rate. This relative increase is consistent with an up-regulation of the cells' photosynthetic apparatus, apparently to provide the additional ATP required by the CCM to increase CO_2 concentrations within the cells and, more importantly, within the chloroplast stroma, the site of CO_2 fixation by RuBisCO. A second line of evidence for up-regulation of the CCM at low CO_2 concentrations was the observed increases in N : C in CO_2-limited cells relative to control values and to N : C under the same decreased growth rate during P limitation (Fig. 7). Such increases were similar for strains CCMP 2228 and CCMP 2229 but were somewhat higher for strain SP3. Increasing cellular N : C with decreasing CO_2 concentrations has also been observed in the diatoms *Thalassiosira pseudonana* and *Thalassiosira weissflogii*, the prymnesiophyte *Isochrysis galbana* (Reinfelder 2012), and a coastal phytoplankton bloom (Tortell et al. 2000). These increases in N : C are consistent with an increased investment of cellular N in proteins within the photosynthetic apparatus needed for the synthesis of ATP, including light-harvesting protein–pigment complexes, ATP biosynthetic proteins, and proteins present within photosynthetic reaction centers and the electron transport chain (Falkowski and Raven 2007). The increase in N : C may also be caused by up-regulation of proteins directly involved in the carbon-concentrating mechanism, such as carbonic anhydrase or bicarbonate uptake proteins (Badger and Price 1994; Sunda and Huntsman 2005). Decreasing CO_2 also can increase the fraction of cellular protein present as RuBisCO (Tortell et al. 2000), so some of the increase in N : C could also be caused by an increase in this central CO_2-fixing protein.

The higher Chl *a* : C and N : C needed to support a given specific growth rate (i.e., a given net C-specific carbon fixation rate) at low CO_2 and high pH in our cultures provides indirect evidence for up-regulation of CCMs and for CO_2 limitation of growth rate. However, we cannot discount the possibility that at least some of the reduction in growth rate is caused directly by the accompanying high pH. This uncertainty will always occur in seawater because pH is determined by chemical equilibria within the carbonate buffer system and, thus, is inherently linked to the CO_2 concentration (Sunda and Cai 2012).

Implications for studying the toxicity of K. brevis *in cultures and field studies*—The results of our experiments have major implications for the accurate measurement of cellular toxin content in dinoflagellates and other toxic algal species and for determining the effect of nutrient limitation on cellular toxins. Typically, the effects of nutrient limitation on cellular toxins are measured in high-density cultures because of the necessity of maintaining sufficiently high cell concentrations to count by microscope accurately. These dense cultures have the advantage of requiring smaller aliquots to measure algal numbers, biomass, growth rates, and toxin levels accurate-

ly. However, our results demonstrate that these high-biomass cultures are likely to be CO_2 limited in many cases, particularly in species with inefficient CCMs or lacking CCMs altogether. This CO_2 limitation can greatly reduce or abrogate toxin responses to nutrient limitation, which might otherwise be apparent in non CO_2-limited cultures. Nutrient limitation effects experiments, therefore, should be conducted in low-density, non–CO_2-limited cultures (Hardison et al. 2012, 2013), and high-density culture experiments should be reserved for examining the effects of growth rate limitation by low CO_2 and high pH or by colimitation by low nutrient and CO_2 concentrations.

Our results also indicate that toxin per cell is a less accurate measure of cell toxin concentrations than is PbTx per unit of cell volume or as a percentage of total cellular carbon. Ironically however, it is the cell toxin parameter most widely reported in the literature (Granéli and Flynn 2006; Sunda et al. 2006).

Our experiments also demonstrate the need for coastal managers and scientists to collect accurate pH measurements during oceanographic cruises examining blooms of *K. brevis* and other phytoplankton. Those measurements can be used to estimate how often and under what environmental conditions blooms are limited by low CO_2 or high pH. These data are crucial for predicting bloom toxicity and understanding when blooms are likely to have the greatest adverse effects on ecosystem services and public health.

Our study further indicates that when *K. brevis* blooms reach sufficiently high cell densities ($\sim$ 5–10 million cells L^{-1}, depending on the strain), the growth demand for CO_2 exceeds the relatively slow rate at which atmospheric CO_2 can diffuse into the water, and growth becomes CO_2-limited (Figs 1–6, panels A; Reinfelder 2011). High-density *K. brevis* blooms can reach cell concentrations of up to 20 million cells L^{-1} (Tester et al. 2008) along the west Florida shelf, where they have caused significant adverse human health, ecological, and economic effects (Hoagland et al. 2009; Fleming et al. 2011). The growth of most high-density *K. brevis* blooms are likely to become either nutrient (Hardison et al. 2012, 2013) or CO_2 limited because of the high biomass demand of the dense blooms for nutrients and CO_2. The results of this and previous studies indicate that the toxin per unit of cell volume or cell carbon is up to twofold greater under P or N limitation than under equivalent CO_2 limitation of growth rate (Fig. 8). Thus, whether a bloom becomes CO_2 or nutrient limited has the potential to influence the toxicity of high density blooms significantly.

Effect of rising atmospheric CO_2 on bloom toxicity—Our findings suggest that ongoing anthropogenic increases in CO_2 concentrations in the atmosphere and surface seawater may promote bloom toxicity by increasing maximum bloom biomass yields. Atmospheric CO_2 concentrations have increased by $\sim$ 42% from the beginning of the industrial era to the present by the burning of fossil fuels and land use changes (Sunda and Cai 2012). If current trends continue, CO_2 levels will increase another twofold by the end of the century (Feely et al. 2009). Equilibration of surface ocean waters with this higher atmospheric P_{CO_2} results in proportional increases in CO_2 concentrations in surface waters and associated increases in TIC. This higher CO_2 and TIC can allow blooms to reach higher biomasses before they become limited by CO_2 or macronutrients, which in turn can lead to higher bloom toxicity. Of course this CO_2-driven increase in bloom biomass will only occur at high nutrient concentrations, where bloom yields are not already limited by nutrients (e.g., N and P) at lower atmospheric P_{CO_2}. Thus, the effect should become increasingly important with increasing concentrations of anthropogenic nutrients in coastal waters, whose levels have risen rapidly in recent decades (Diaz and Rosenberg 2008; Sunda and Cai 2012).

The effect of increasing CO_2 on bloom biomass has been shown experimentally in cultures of the toxic diatom *P. multiseries* grown in nutrient-sufficient batch cultures, where an increase in CO_2 concentrations linked to a decrease in culture pH from 8.6 to 8.0, caused a 2.5-fold increase in final cell yield (Lundholm et al. 2004). The effect of past and future anthropogenic increases in atmospheric P_{CO_2} on biomass yields of nutrient-sufficient *K. brevis* blooms can be estimated from our batch culture data (*see* Methods). The current atmospheric (P_{CO_2}) is $\sim$ 41 Pa (400 ppm), whereas it was 28 Pa in preindustrial times and is expected to rise to $\sim$ 81 Pa by the end of this century (Feely et al. 2009; Sunda and Cai 2012). The equivalent equilibrium TIC values for seawater at our experimental salinity (36), alkalinity (2.35 mmol kg^{-1}), and temperature (23°C) are 1.976, 2.054, and 2.185 mmol kg^{-1}, respectively, at these three P_{CO_2} values (28, 41, and 81 Pa). Growth ceased in our CO_2-limited batch cultures of *K. brevis* at pH 9.0, which based on equilibrium calculations (Sunda and Cai 2012) is associated with computed TIC values of 1.463–1.467 mmol kg^{-1}, depending on the computed amount of C fixation (*see* below) and associated small variations in total alkalinity (2.40–2.42 μmol kg^{-1}) caused by nitrate assimilation (*see* Methods). Based on these values, the amount of CO_2 consumed by photosynthetic C fixation in *K. brevis* before growth was completely stopped by insufficient CO_2 would be 0.513 mmol kg^{-1} at the preindustrial P_{CO_2} (28 Pa), 0.586 mmol kg^{-1} at the current P_{CO_2} (41 Pa), and 0.708 mmol kg^{-1} at the projected P_{CO_2} for year 2100 (81 Pa). This amounts to a 14% higher maximum bloom carbon yield at the current P_{CO_2} (41 Pa) and a 38% higher yield at the turn of the century P_{CO_2} (81 Pa) relative to the bloom yield in preindustrial times.

As a check on the validity of these calculations, we compared our computed CO_2-limited carbon yields at pH 9.0 for the current atmospheric P_{CO_2} with experimental measurements of cell carbon in our CO_2-limited cultures at the same pH. To do this we first regressed our cell carbon measurements (mol kg^{-1} culture) vs. pH in the CO_2-limited range of pH (8.85–9.08) for all CO_2-limited cultures of all three *K. brevis* strains. Based on the regression line (r^2 = 0.90), we obtained a cellular carbon value of 0.605 mmol kg^{-1} for the CO_2-limited pH 9.0 cultures. This value is within 3% of our modeled fixed carbon value at that pH (0.586 mmol kg^{-1}) at the current atmospheric P_{CO_2}.

Higher atmospheric CO_2 concentrations may also increase bloom toxicity by increasing the likelihood that the growth of *Karenia* blooms will become N or P limited at high bloom biomass rather than CO_2 limited. This effect should increase bloom toxicity because our data show that N- or P-limited cells have higher brevetoxin to cell carbon ratios than those that are limited by low CO_2. Thus, N- or P-limited blooms should have higher brevetoxin concentrations than CO_2-limited blooms for a given bloom biomass.

A final factor that may increase bloom toxicity is the complex response of nutrient-limited cells to increasing atmospheric CO_2 levels. As noted earlier, P- and Si-limited cultures of *Pseudo-nitzschia* exhibited much larger increases in the cellular toxin domoic acid when exposed to elevated P_{CO_2} than when exposed to current or preindustrial P_{CO_2} values (Sun et al. 2011; Tatters et al. 2012). If such behavior is widespread in other toxic species, it should also promote higher bloom toxicity in a future high-CO_2 world.

Together these three potential effects of higher CO_2 concentrations—higher bloom biomass yields, an increased likelihood of N- or P-limited blooms, and a greater increase in cellular toxins under nutrient limitation of growth rate—could substantially increase bloom toxicity and result in increased adverse effects on human heath, coastal ecosystems, and coastal economies. These effects are likely already occurring to some extent given the current 42% higher levels of atmospheric CO_2 due to man's activities compared with preindustrial times and will only worsen in the future with continuing anthropogenic increases in atmospheric CO_2.

Acknowledgments

We thank Ed Buskey for provision of strain SP3, Dave Eggelston for infrastructure support, and Dan Kamykowski for insightful discussions. We also thank Andrea Bourdelais and Daniel Baden for assistance in brevetoxin extractions and two anonymous reviewers whose helpful suggestions improved the manuscript.

References

Backer, L. C. 2009. Impacts of Florida red tides on coastal communities. Harmful Algae **8:** 618–622, doi:10.1016/j.hal.2008.11.008

Badger, M. R., and G. D. Price. 1994. The role of carbonic anhydrase in photosynthesis. Annu. Rev. Plant Biol. **45:** 369–392.

Brand, L. E., L. Campbell, and E. Bresnan. 2012. *Karenia*: The biology and ecology of a toxic genus. Harmful Algae **14:** 156–178, doi:10.1016/j.hal.2011.10.020

Bryant, J. P., F. S. Chapin, and D. R. Klein. 1983. Carbon/nutrient balance of boreal plants in relation to vertebrate herbivory. Oikos **40:** 357–368, doi:10.2307/3544308

Cheng, Y. S., and others. 2005. Characterization of marine aerosol for assessment of human exposure to brevetoxins. Environ. Health Perspect **113:** 638–643, doi:10.1289/ehp.7496

Cohen, J. H., P. A. Tester, and R. B. Forward. 2007. Sublethal effects of the toxic dinoflagellate *Karenia brevis* on marine copepod behavior. J. Plankton Res. **29:** 301–315, doi:10.1093/plankt/fbm016

Diaz, R. J., and R. Rosenberg. 2008. Spreading dead zones and consequences of marine ecosystems. Science **321:** 926–929, doi:10.1126/science.1156401

Falkowski, P. G., and J. A. Raven. 2007. Aquatic photosynthesis, 2nd ed. Princeton Univ. Press.

Feely, R. A., S. C. Doney, and S. R. Cooley. 2009. Ocean acidification: Present conditions and future changes in a high-CO_2 world. Oceanography **22:** 36–47, doi:10.5670/oceanog.2009.95

Fleming, L. E., and others. 2011. Review of Florida red tide and human health effects. Harmful Algae **10:** 224–233, doi:10.1016/j.hal.2010.08.006

Flewelling, L. J., and others. 2005. Red tides and marine mammal mortalities. Nature **435:** 755–756, doi:10.1038/nature435755a

Giordano, M., J. Beardall, and J. A. Raven. 2005. CO_2 concentrating mechanisms in algae: Mechanisms, environmental modulation, and evolution. Annu. Rev. Plant Biol. **56:** 99–131, doi:10.1146/annurev.arplant.56.032604.144052

Granéli, E., and K. Flynn. 2006. Chemical and physical factors influencing toxin content, p. 229–241. *In* E. Granéli and J. T. Turner [eds.], Ecology of harmful algae. Springer.

Hansen, P. J. 2002. Effect of high pH on the growth and survival of marine phytoplankton: Implications for species succession. Aquat. Microb. Ecol. **28:** 279–288, doi:10.3354/ame028279

Hardison, D. R., W. G. Sunda, R. W. Litaker, D. Shea, and P. A. Tester. 2012. Nitrogen limitation increases brevetoxins in *Karenia brevis* (Dinophyceae): Implications for bloom toxicity. J. Phycol. **48:** 844–858, doi:10.1111/j.1529-8817.2012.01186.x

———, ———, D. Shea, and R. W. Litaker. 2013. Increased toxicity of *Karenia brevis* during phosphate limited growth: Ecological and evolutionary implications. Plos One **8:** e58545, doi:10.1371/journal.pone.0058545

Hay, M. E., and W. Fenical. 1988. Marine plant–herbivore interactions: The ecology of chemical defense. Annu. Rev. Ecol. Syst. **19:** 111–145, doi:10.1146/annurev.es.19.110188.000551

Hoagland, P., and others. 2009. The costs of respiratory illnesses arising from Florida gulf coast *Karenia brevis* blooms. Environ. Health Perspect. **117:** 1239–1243, doi:10.1289/ehp.0900645

———, and S. Scatasta. 2006. The economic effects of harmful algal blooms, p. 391–402. *In* E. Graneli and J. T. Turner [eds.], Ecology of harmful algae. Springer.

Hong, J., S. Talapatra, J. Katz, P. A. Tester, R. J. Waggett, and A. R. Place. 2012. Algal toxins alter copepod feeding behavior. Plos One **7:** e36845, doi:10.1371/journal.pone.0036845

Ianora, A., and others. 2006. New trends in marine chemical ecology. Estuar. Coasts **29:** 531–551.

Keller, M. D., W. K. Bellows, and R. R. L. Guillard. 1988. Microwave treatment for sterilization of phytoplankton culture media. J. Exp. Mar. Biol. Ecol. **117:** 279–283, doi:10.1016/0022-0981(88)90063-9

Lee, K. L., and others. 2006. Global relationships of total alkalinity with salinity and temperature in surface waters of the world's oceans. Geophys. Res. Lett. **33:** L19605, doi:10.1029/2006GL027207

Lekan, D. K., and C. R. Tomas. 2010. The brevetoxin and brevenal composition of three *Karenia brevis* clones at different salinities and nutrient conditions. Harmful Algae **9:** 39–47, doi:10.1016/j.hal.2009.07.004

Lundholm, N., P. J. Hansen, and Y. Kotaki. 2004. Effect of pH on growth and domoic acid production by potentially toxic diatoms of the genera *Pseudo-nitzschia* and *Nitzschia*. Mar. Ecol. Prog. Ser. **273:** 1–15, doi:10.3354/meps273001

Mendoza, W. G., R. N. Mead, L. E. Brand, and D. Shea. 2008. Determination of brevetoxin in recent marine sediments. Chemosphere **73:** 1373–1377, doi:10.1016/j.chemosphere.2008.07.089

Niyogi, K. 1999. Photoprotection revisited: Genetic and molecular approaches. Annu. Rev. Plant Biol. **50:** 333–359.

Reinfelder, J. R. 2011. Carbon concentrating mechanisms in eukaryotic marine phytoplankton. Ann. Rev. Mar. Sci. **3:** 291–315, doi:10.1146/annurev-marine-120709-142720

———. 2012. Carbon dioxide regulation of nitrogen and phosphorus in four species of marine phytoplankton. Mar. Ecol. Prog. Ser. **466:** 57–67, doi:10.3354/meps09905

Riebesell, U., D. Wolf-Gladrow, and V. Smetacek. 1993. Carbon dioxide limitation of marine phytoplankton growth rates. Nature **361:** 249–251, doi:10.1038/361249a0

Rost, B., K. Richter, U. Riebelsell, and P. J. Hansen. 2006. Inorganic carbon acquisition by red tide dinoflagellates. Plant Cell Environ. **29:** 810–822, doi:10.1111/j.1365-3040.2005.01450.x

Schmidt, L. E., and P. J. Hansen. 2001. Allelopathy in the prymnesiophyte *Chrysochromulina polylepis:* Effect of cell concentration, growth phase and pH. Mar. Ecol. Prog. Ser. **216:** 67–81, doi:10.3354/meps216067

Sun, J., D. A. Hutchins, Y. Feng, E. L. Seubert, D. A. Caron, and F.-X. Fu. 2011. Effects of changing P_{CO_2} and phosphate availability on domoic acid production and physiology of the marine harmful bloom diatom *Pseudo-nitzschia multi-series*. Limnol. Oceanogr. **56:** 829–840, doi:10.4319/lo.2011.56.3.0829

Sunda, W. G., and W. J. Cai. 2012. Eutrophication induced CO_2-acidification of subsurface coastal waters: Interactive effects of temperature, salinity, and atmospheric P_{CO_2}. Environ. Sci. Technol. **46:** 10,651–10,659, doi:10.1021/es300626f

———, E. Graneli, and C. J. Gobler. 2006. Positive feedback and the development and persistence of ecosystem disruptive algal blooms. J. Phycol. **42:** 963–974, doi:10.1111/j.1529-8817.2006.00261.x

———, and D. R. Hardison. 2010. Evolutionary tradeoffs among nutrient acquisition, cell size, and grazing defense in marine phytoplankton promote ecosystem stability. Mar. Ecol. Prog. Ser. **401:** 63–76, doi:10.3354/meps08390

———, R. Hardison, R. P. Kiene, E. Bucciarelli, and H. Harada. 2007. The effect of nitrogen limitation on cellular DMSP and DMS release in marine phytoplankton: Climate feedback implications. Aquat. Sci. **69:** 341–351, doi:10.1007/s00027-007-0887-0

———, and S. A. Huntsman. 2005. Effect of CO_2 supply and demand on zinc uptake and growth limitation in a coastal diatom. Limnol. Oceanogr. **50:** 1181–1192, doi:10.4319/lo.2005.50.4.1181

———, N. M. Price, and F. M. Morel. 2005. Trace metal ion buffers and their use in culture studies, p. 35–63. *In* R. A. Andersen [ed.], Algal culturing techniques. Elsevier Academic.

Tatters, A. O., F. X. Fu, and D. A. Hutchins. 2012. High CO_2 and silicate limitation synergistically increase the toxicity of *Pseudo-nitzschia fraudulenta*. Plos One **7:** e32116, doi:10.1371/journal.pone.0032116

Tester, P. A., D. Shea, S. R. Kibler, S. M. Varnam, M. D. Black, and R. W. Litaker. 2008. Relationships among water column toxins, cell abundance and chlorophyll concentrations during *Karenia brevis* blooms. Cont. Shelf Res. **28:** 59–72, doi:10.1016/j.csr.2007.04.007

Tortell, P. D., G. H. Rau, and F. M. Morel. 2000. Inorganic carbon acquisition in coastal Pacific phytoplankton communities. Limnol. Oceanogr. **45:** 1485–1500, doi:10.4319/lo.2000.45.7.1485

Trimborn, S., N. Lundholm, S. Thoms, K. U. Richter, B. Krock, P. J. Hansen, and B. Rost. 2008. Inorganic carbon acquisition in potentially toxic and non-toxic diatoms: The effect of pH-induced changes in seawater carbonate chemistry. Physiol. Plant. **133:** 92–105, doi:10.1111/j.1399-3054.2007.01038.x

Ulitzur, S., and M. Shilo. 1964. A sensitive assay system for determination of the ichthyotoxicity of *Prymnesium parvum*. J. Gen. Microbiol. **36:** 161–169, doi:10.1099/00221287-36-2-161

———, and ———. 1966. Mode of action of *Prymnesium parvum* ichthyotoxin. J. Eukaryot. Microbiol. **13:** 332–336.

Vargo, G. A. 2009. A brief summary of the physiology and ecology of *Karenia brevis* Davis (G. Hansen and Moestrup comb. nov.) red tides on the West Florida Shelf and of hypotheses posed for their initiation, growth, maintenance, and termination. Harmful Algae. **8:** 573–584, doi:10.1016/j.hal.2008.11.002

Waggett, R. J., D. R. Hardison, and P. A. Tester. 2012. Toxicity and nutritional inadequacy of *Karenia brevis*: Synergistic mechanisms disrupt top-down grazer control. Mar. Ecol. Prog. Ser. **444:** 15–30, doi:10.3354/meps09401

Watkins, S. M., A. Reich, L. E. Fleming, and R. Hammond. 2008. Neurotoxic shellfish poisoning. Mar. Drugs **6:** 431–455, doi:10.3390/md20080021

Welschmeyer, N. A. 1994. Fluorometric analysis of chlorophyll *a* in the presence of chlorophyll *b* and pheopigments. Limnol. Oceanogr. **39:** 1985–1992, doi:10.4319/lo.1994.39.8.1985

Associate editor: Heidi M. Sosik

Received: 14 June 2013
Accepted: 13 November 2013
Amended: 12 December 2013